Journal of Power Sources 184 (2008) 385–391

Contents lists available at ScienceDirect

Journal of Power Sources

journal homepage: www.elsevier.com/locate/jpowsour

High yield hydrogen production from low CO selectivity ethanol steam reforming over modified Ni/Y_2O_3 catalysts at low temperature for fuel cell application

Jie Sun [1,*], Dingfa Luo [3], Pu Xiao [2], Li Jigang [1], Shanshan Yu [2]

[1] *Lab of Renewable Energy and Energy Safety, Institute of Chemical Defense, Beijing 102205, China*
[2] *Department of Chemistry, Tsinghua University, Beijing 100084, China*
[3] *Department of Chemistry, Xinyang Normal University, Xinyang 464000, China*

ARTICLE INFO

Article history:
Received 29 December 2007
Received in revised form 17 February 2008
Accepted 29 February 2008
Available online 14 March 2008

Keywords:
Hydrogen production
Low CO selectivity
Ethanol steam reforming
Fuel cell

ABSTRACT

Ethanol–water mixtures were converted directly into H_2 with 67.6% yield and >98% conversion by catalytic steam reforming at 350 °C over modified Ni/Y_2O_3 catalysts heat treated at 500 °C. XRD was used to test the structure and calculate the grain sizes of the samples with different scan rates. The initial reaction kinetics of ethanol over modified and unmodified Ni/Y_2O_3 catalysts were studied by steady state reaction and a first-order reaction with respect to ethanol was found. TPD was used to analyze mechanism of ethanol desorption over Ni/Y_2O_3 catalyst. Rapid vaporization, efficiency tube reactor and catalyst were used so that homogeneous reactions producing carbon, acetaldehyde, and carbon monoxide could be minimized. And even no CO detective measured during the first 49 h reforming test on the modified catalyst Ni/Y_2O_3. This process has great potential for low cost H_2 generation in fuel cells for small portable applications where liquid fuel storage is essential and where systems must be small, simple, and robust.

1. Introduction

Cellulose ethanol was selected to be the candidate hydrogen fuel for its properties well fit with the requirements of safe handling, cheap, and easy transport, low toxicity and biodegradability. During cellulose ethanol to hydrogen production processes, the reactions between CO_2 and biomass show a renewable energy cycle: $C_6H_{12}O_6 \rightarrow 2C_2H_5OH + 2CO_2 \rightarrow 10H_2 \rightarrow 20e^-$. Photosynthesis first converts CO_2 and H_2O into carbohydrates and sugars, represented here as glucose, $C_6H_{12}O_6$. In the reaction sequence through ethanol, fermentation converts glucose into ethanol and CO_2. Furthermore, the cost of production of aqueous ethanol, as required in the hydrogen production process, is significantly lower than the cost of anhydrous ethanol which is required in internal combustion engines [1,2].

Many reactions of ethanol over metals and metal oxides have been investigated in recent years. Reactions of ethanol dehydrogenation over noble metal membrane [3–5], and reactions of ethanol over M/CeO_2 catalysts [6–8] have been studied. The catalytic properties of the supported transition metal catalysts to one of the steam reforming reactions (reaction (2)) show that the selectivity of H_2 for the reforming reaction is in the order: Co much greater than Ni > Rh > Pt, Ru, Cu [9–12]. The studies of ethanol steam reforming in a molten carbonate fuel cell (MCFC) utilized the catalysts from the noble metals (Pt, Rh, etc.) to CuO/ZnO/Al_2O_3, NiO/CuO/SiO_2, Ni/MgO and Co/MgO, they got good results: the selectivity of hydrogen of 5%Rh/Al_2O_3 can reach to 30.1 vol.% [13–16]. The steam reforming of ethanol at about 300 °C over catalyst of Cu/Ni/K/γ-Al_2O_3 was also studied [17,18].

In recent researches, nickel catalysts were widely studied for their good activity in ethanol steam reforming and low cost [1,19–23]. Ni/Al_2O_3 catalysts had been reported to be the most effective catalysts for reforming of methane with carbon dioxide, but they suffer a serious problem of carbon deposition, nickel sintering and phase transformation [24–26]. It was well known that rare earth metal oxides were of high alkalinity and were favorable for dehydrogenation of alcohols. Ni/La_2O_3 catalyst had been previously found to exhibit good performance under conditions (800 °C) of reforming of methane with carbon dioxide, and to be very active and stable for the steam reforming of ethanol under certain operating conditions (above 300 °C) [19,27], while Y_2O_3 was more active for dehydrogenation than oxides of other elements in La system.

The reactions of ethanol steam reforming include 3 major reactions of the production of H_2, CO_2, CO and CH_4.

$$C_2H_5OH + 3H_2O \rightarrow 2CO_2 + 6H_2, \quad \Delta H^0_{298} = +174\,\text{kJ mol}^{-1} \qquad (1)$$

* Corresponding author. Tel.: +8610 66757029 82140; fax: +8610 52565168.
E-mail address: magnsun@mail.tsinghua.edu.cn (J. Sun).

0378-7753/$ – see front matter © 2008 Elsevier B.V. All rights reserved.
doi:10.1016/j.jpowsour.2008.02.092

$$C_2H_5OH + H_2O \rightarrow 2CO + 4H_2, \quad \Delta H^0_{298} = +256\,kJ\,mol^{-1} \quad (2)$$

$$C_2H_5OH + 2H_2 \rightarrow 2CH_4 + H_2O, \quad \Delta H^0_{298} = -157\,kJ\,mol^{-1} \quad (3)$$

From the thermodynamics, higher temperature favored to form CO while lower temperature favored to CH_4 [20]. The equilibrium yield rate of H_2 (Y_{H_2}) could be possibly affected by 3 major parameters, equilibrium temperature (T), total pressure (P), and initial molal ratio of H_2O/ethanol (R). Y_{H_2} increased with the increasing of T and R, while decreased with the increasing of P. For example, when $P = 1$ bar and $R = 3$, Y_{H_2} could reach the maximum at 700 °C. But sometime suitable increase in pressure was necessary, the work pressure needed to be 8–15 bar for Pd–Ag membrane reactor.

Another 5 reactions also happened in ethanol steam reforming process:

$$C_2H_5OH \rightarrow CH_3CHO + H_2, \quad \Delta H^0_{298} = +68\,kJ\,mol^{-1} \quad (4)$$

$$C_2H_5OH \rightarrow C_2H_4 + H_2O, \quad \Delta H^0_{298} = +45\,kJ\,mol^{-1} \quad (5)$$

$$CH_4 + 2H_2O \rightarrow CO_2 + 4H_2, \quad \Delta H^0_{298} = +166\,kJ\,mol^{-1} \quad (6)$$

$$C_2H_5OH \rightarrow CO + CH_4 + H_2, \quad \Delta H^0_{298} = +49\,kJ\,mol^{-1} \quad (7)$$

$$CO + H_2O \rightarrow CO_2 + H_2, \quad \Delta H^0_{298} = -41\,kJ\,mol^{-1} \quad (8)$$

Many researches indicated that acetaldehyde and ethylene would be formed before the formation of H_2 and CO_X in reactions (1) and (2) under relative low temperature. The dehydrogenation and dehydration of ethanol were much faster than the steam reforming of ethanol. So, acetaldehyde and ethylene were thought as important intermediate products in the steam reforming reactions [20,22,28]. Then, the support of catalyst would be a key role. (i) It should favor H_2O molecules break to OH groups, and accelerate these active particles to transfer to metal particles and form final products of CO_X and H_2 [29–31]; (ii) it could catalyze reactions (4) and (5), and affected selectivity of final product [18,20,23,32–34]; (iii) it could contribute to the stability of metal particles under high temperature [35–41]. Thermodynamics claimed when $T > 200$ °C, reaction (7) will be favored. At higher temperatures, the methane yield is reduced via the CH_4 steam reforming reaction (6). But the high temperature will cause the sinter of catalysts and coke formation. There were a couple of contradictions. Reaction (8) could decrease CO and increase H_2, it was favored at temperature range 200–400 °C. So, we hope to combine the WGS reaction and the reforming reaction at an appropriate temperature to eliminate CO.

In most of our works, the choice of supports was focused on the rare earth metal oxides for their high alkalinity and favor of dehydrogenation of alcohols. We, however, used nickel with supports (yttria, lanthanum oxide, ceria, zirconia, low-area alumina, etc.) [21,22,42,43] as catalysts for ethanol steam reforming reactions. In this work, Ni/Y_2O_3 was modified through heat treatment to eliminate CO and increase H_2 selectivity, considering its good low temperature activity for ethanol steam reforming [21,22,42].

2. Experimental

The catalysts of nickel with yttria for ethanol steam reforming reaction were deposited from salt solutions [22].

X-ray powder diffraction (XRD) was carried out on a Rigaku X-ray diffraction equipment, using the Cu Kα radiation, at 40 kV and 20 mA.

The heat treatment was carried out in a programmed oven from 450 °C (sample T_1) to 900 °C (sample T_{10}), the heat rate was 10 °C min^{-1}, and the sample was kept at the aim temperature for 4 h after the aim temperature was reached. The precursor for all the samples was NiC_2O_4/Y_2O_3. For example, for sample T_1, the precursor NiC_2O_4/Y_2O_3 was heated from room temperature to 450 °C, heat rate 10 °C min^{-1}, when temperature reached 450 °C the sample was kept at 450 °C for 4 h, then cooled down to room temperature naturally, then sample T_1 was formed.

Before the steam reforming test, catalyst was deoxidized in H_2 at 450 °C for 2 h and then cool down to room temperature. Steam reforming test was carried out on a self-built system. Ethanol–water mixtures were injected into a tube through an electronically controlled sprayer-slide that sprayed small droplets onto the walls of the tube, heated to 200 °C. This produced rapid vaporization, so that reactants went from liquids at room temperature to products exiting the catalyst in less than 46 ms.

Products were analyzed by a gas chromatography Angilent 7890A with 2 TCDs, with mass balances closing to within 0.1%. All experiments were run for up to 60 h on a given catalyst, and most experiments were repeated on several catalysts. No significant deactivation or variations between catalysts were noted in these experiments.

Kinetic analysis was conducted with a fixed-bed reactor with inner diameter of 6 mm fitted in a programmable oven, with an operating range up to 700 °C and linked to a gas chromatograph (GC-14C) via a six-way valve. Ethanol in a saturator at 0 °C was introduced via a continuous flow of nitrogen. The GC was equipped with a thermal conductive detector (TCD) coupled to a PC. A packed column (Porapak, 80–100 mesh, 1.5 m long) was used for the separation of organic compounds (such as C_2H_5OH, H_2O and CH_3CHO) at 100 °C with H_2 as carrier gas. The gas, containing ethanol, was allowed to flow over the catalyst for 10 min at room temperature before samples were injected into the GC via the six-way valve. Several runs were done in order to obtain a consistent result for ethanol peak area. Several runs were then performed with varying flow rates and reaction temperatures. For Arrhenius plots, ethanol conversion was kept at <20%. Water, ethanol and acetaldehyde were the only observed products below 150 °C.

Temperature programmed desorption (TPD) test was carried out on a Quantachrom Instruments Autosorb-1. An OmniStar™ Qms-2000 mass spectrometer coupled to a PC with software for acquisition of mass peak data was used to analyze the effluent. Prior to adsorption, the catalyst sample was dried at 100 °C for 1 h then cooled down to room temperature and then was put into the sample cell of a sorption instrument to adsorb ethanol for 1 h at room temperature. Then the sample was taken out from the sample cell of sorption instrument and put in the capillary of the Autosorb-1 to carry out TPD test. The vacuum was up to 10^{-6} Torr, the catalyst temperature was raised from 50 to 650 °C at a rate of 15 °C min^{-1}. The mass spectrometer used in this study was limited to monitor 50 masses/cycles. To identify a product from mass spectral data, knowledge of the fragmentation pattern is required. Such patterns can be easily obtained by scanning the mass range of interest while leaking the desired gas into the vacuum system. However, lists of fragmentation patterns for numerous compounds are readily available. The relative yields of the desorption products were determined following the techniques used by other researchers [6–8].

3. Results and discussion

3.1. XRD and heat treatments

Fig. 1 shows the XRD patterns of catalysts Ni/Y_2O_3 samples with different heat-treated temperatures from 350 to 800 °C at scan rate of 8° min^{-1}. The strength of peaks increased with the increase of heat-treated temperature, and the diffraction peaks of NiO transfer to high degree direction regularly. The diffraction peaks of Y_2O_3 also transfer to high degree. The peaks labeled with the symbol "*"are corresponding to the diffraction of NiO. There are no new peaks appearing in the XRD patterns of Ni/Y_2O_3, means that the catalysts

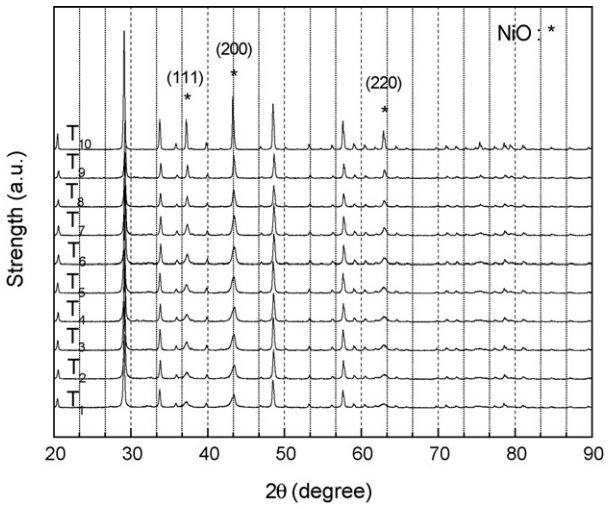

Fig. 1. XRD of the samples treated at different temperatures.

were just the mixture of nickel and its supports and no new phase was formed.

From the diffraction peaks of NiO (2 2 0), as shown in Fig. 2, at low scan rate of 1° min^{-1} from 60–65°, the diffraction peaks of Y_2O_3 (8 2 2), as shown in Fig. 3, at low scan rate of 1° min^{-1} from 77–82°, the crystal grain sizes of NiO, Y_2O_3 in sample T_4–T_9, calculated with Scherrer formula were shown in Fig. 4. The grain sizes of NiO increased with heat-treated temperature, and the increasing rate was much larger when the temperature was above 650 °C. The grain sizes of Y_2O_3 did not change obviously below 750 °C because finished product of Y_2O_3 was used as support precursor which has a melting point much higher than 2000 °C. So, the Tamman temperature of Ni/Y_2O_3 catalyst should be closed to 650 °C. If the heat-treated temperature is above 650 °C, the grain sizes of catalyst Ni/Y_2O_3 would increase quickly, and the micropores of the catalysts would be sintered or semi-melted, which leads to the decrease of the activity of catalysts directly.

3.2. Catalysts activity and selectivity

We defined ethanol conversion (C_E) and product selectivity (S_P) as:

$$S_P = \frac{\text{mol}_p}{\text{mol}_{sp}} \times 100\% \quad (9)$$

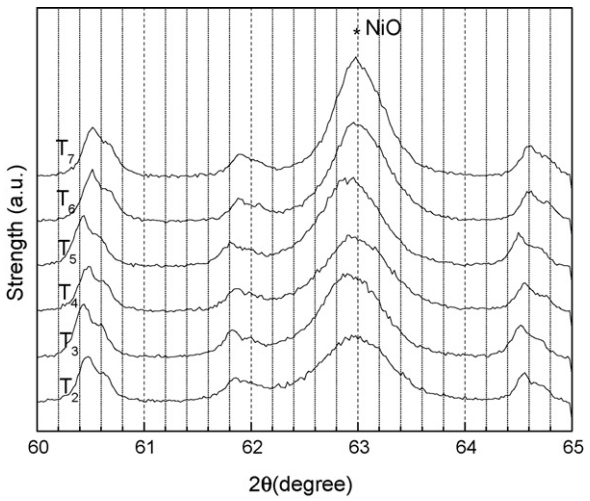

Fig. 2. Character patterns of NiO in T_2–T_7 samples XRD.

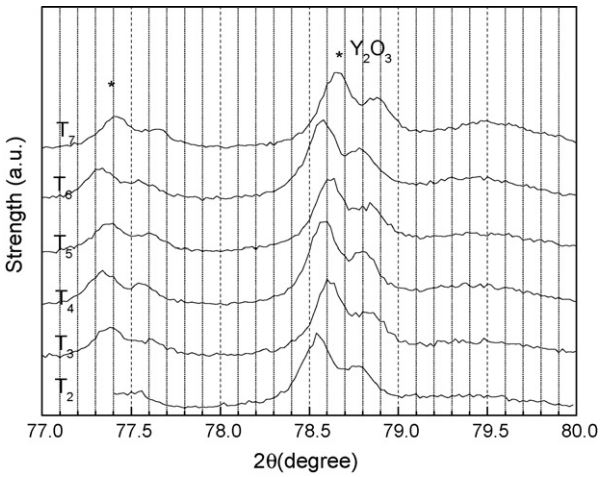

Fig. 3. Character patterns of Y_2O_3 in T_2–T_7 samples XRD.

$$C_{EtOH} = \frac{C_{in} - C_{out}}{C_{in}} \times 100\% \quad (10)$$

Because the H atoms from H_2O can also be converted into H_2, Y_{H_2} was defined as the fraction of H in the ethanol and water molecules converted into H_2. So, complete conversion of the ethanol and water from the steam reforming reaction (1) could generate 6 H_2 per C_2H_5OH, which gives a maximum H_2 yield of 100%. Three H_2 molecules from C_2H_5OH represent 50% Y_{H_2} only.

Typical results of ethanol reforming on Ni–yttria are shown in Fig. 5, in which the selectivity of each product and the conversion of ethanol are shown as a function of reaction temperature in the low-temperature range of 250–350 °C. These experiments were done at a total flow rate of 6.8 standard l min^{-1} [gas hourly space velocity (GHSV) ~7.8×10^4 h^{-1}], with preheating to 200 °C.

Fig. 5 shows that at a temperature of 250 °C, steam reforming of ethanol occurred obviously over the catalyst Ni/Y_2O_3, the ethanol conversion reached 81.9%, and the selectivity of hydrogen, methane, carbon dioxide and carbon monoxide was 43.1%, 20.9%, 9.7% and 26.3%, respectively. A small amount of acetaldehyde was also detected with a selectivity of 0.7%. When the temperature increased from 250 to 320 °C, the conversion of ethanol increased to 95.3%, the selectivity of hydrogen increased to the maximal value 53.6%, indicating that the water-gas shift reaction of carbon monoxide has occurred. In the temperature range of 320–350 °C, the

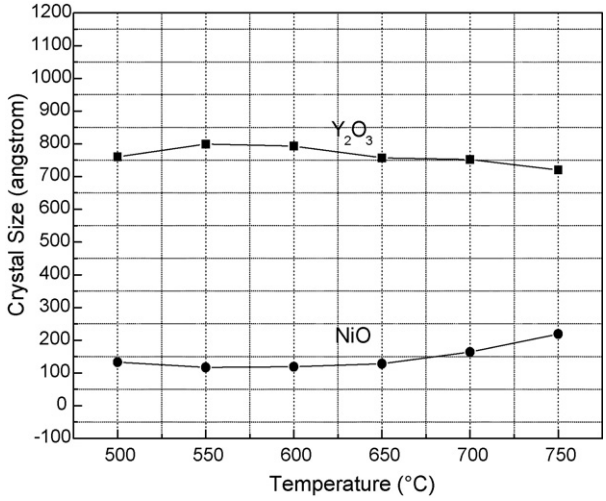

Fig. 4. The effect of temperature on the grain sizes of Y_2O_3 and NiO.

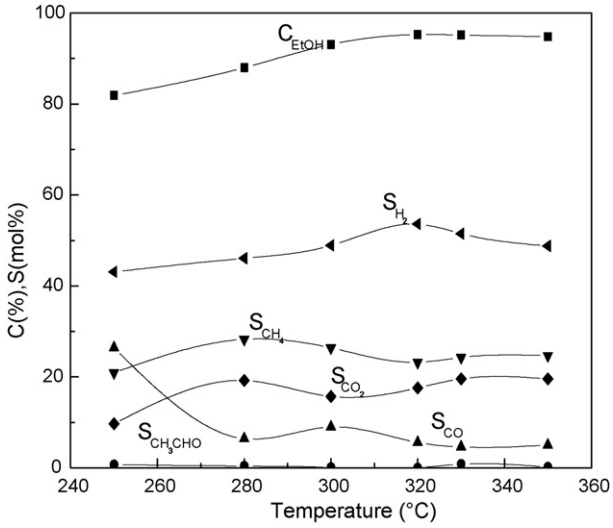

Fig. 5. Effect of reaction temperature T on conversion of ethanol (C_{EtOH}) and on selectivity of hydrogen (S_{H_2}), carbon monoxide (S_{CO}), carbon dioxide (S_{CO_2}), methane (S_{CH_4}) and acetaldehyde (S_a) obtained over the catalyst Ni/Y_2O_3 reduced by hydrogen for 2 h at 450 °C. Experimental conditions: mass of catalyst 4 g, particle size 0.5–1 mm, H_2O/EtOH mol ratio R = 3:1, liquid flow rate 0.05 $cm^3\ min^{-1}$, total flow rate of 6.8 standard l min^{-1} gas hourly space velocity (GHSV) ~$7.8 \times 10^4\ h^{-1}$, P = 1 atm.

selectivity of acetaldehyde reached 0.2%, the selectivity of hydrogen decreased to 48.9%, while the selectivity of methane and carbon dioxide increased to 25.8% and 19.7%. The conversion of ethanol has reached to 95.3% at 320 °C. This high result means very good activity of the Ni/Y_2O_3 catalyst, which is much better than Ni/Al_2O_3 in this temperature domain [21].

The stability of catalysts Ni/Y_2O_3 with time-on-stream was examined for 60 h at a temperature of 320 °C. The relationships of selectivity of each product and conversion of ethanol with time-on-stream were shown in Fig. 6. For catalyst Ni/Y_2O_3, under the experimental conditions, the conversion of ethanol was about 93%. The selectivity of hydrogen obviously increased during the first

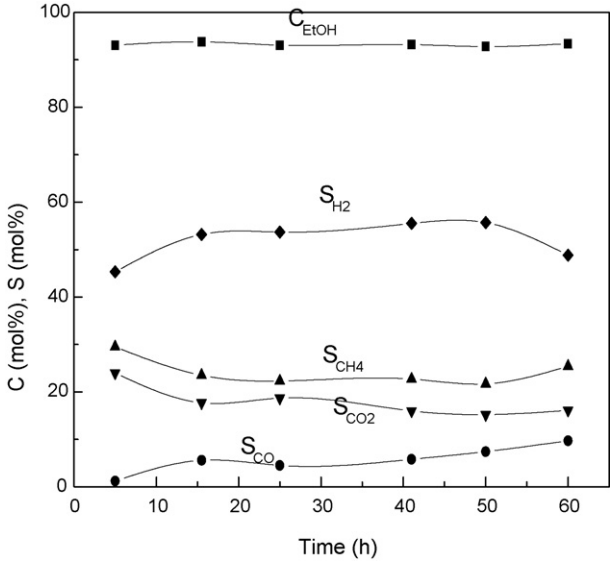

Fig. 6. Conversion of ethanol and selectivity of products as function of time-on-stream, obtained over the Ni/Y_2O_3 catalyst. Experimental conditions: mass of catalyst 4 g, H_2O/EtOH mol ratio R = 3:1, liquid flow rate 0.05 $cm^3\ min^{-1}$, total flow rate of 6.8 standard l min^{-1} gas hourly space velocity (GHSV) ~$7.8 \times 10^4\ h^{-1}$, T = 320 °C, P = 1 atm.

15 h from 45.3% to 53.2% and kept stable during the 15–50 h, then decreased lightly during the last 10 h.

The activity, product selectivities and stability with time-on-stream of modified catalyst Ni/Y_2O_3 sample T_2, T_3 and T_5 were shown in Tables 1, 2 and 3. The low temperature activity and CO elimination ability of Ni/Y_2O_3 catalyst were improved more through sample T_2. The selectivity of hydrogen still kept 64.9 vol.% after 79 h reforming test. But the H_2 selectivity and stability at low temperature of sample T_3 and T_5 was much lower than T_2. At 350 °C, the highest H_2 selectivity of sample T_3 and T_5 was 54.1 and 50.7 vol.%, respectively, while the mean value of H_2 selectivity of sample T_2 was about 64.4 vol.% during the 79 h test. The highest H_2 selectivity of sample T_3 and T_5 at 500 °C was 63.1 and 55.0 vol.%, respectively, which was still lower than the mean value of H_2 selectivity (64.4 vol.%) of sample T_2 at 350 °C. So, the test results showed obviously that sample T_2 treated at 500 °C with NiO grain size of 13.3 nm and Y_2O_3 of 76 nm is the best for ethanol reforming. The results of sample T_2 for ethanol reforming were also better than Ni/La_2O_3 in same temperature domain [21] and some rare metal supported catalysts [16].

Through controlling of reforming temperature range to match the WGS reaction temperature range, the CO selectivity was decreased evidently, as shown in Table 1. The catalyst was very stable during a 79 h steam reforming test at 350 °C, with high H_2 selectivity, 68.7 vol.% and high Y_{H_2} (67.6%, consider of total H atoms in C_2H_5OH and H_2O molecules, 119.8%, consider of H atoms in C_2H_5OH molecules only). And in the first 49 h, no CO detected. The results indicated that heat treatment at 500 °C had active effects on catalyst.

In the process of heat treatment on catalyst Ni/Y_2O_3, the grain sizes changed, the pore structure of the catalysts was reconstructed, which led to the change of surface area finally. Heat stability of aperture structure of the support follows: micropore of 0–10 nm stable below 500 °C, transition pore of 10–200 nm stable between 500 and 800 °C. So, micropore and transition pore of sample T_2 (heat treated at 500 °C) could be kept. However, micropore of sample T_3 (heat treated at 550 °C) and T_5 (heat treated at 650 °C) had been sintered. The heat-treatment temperature was higher, the sintering was more seriously. So, the H_2 selectivity and stability of the catalysts followed the order: T_2 > unmodified Ni/Y_2O_3 > T_3 > T_5.

Why sample T_2 had the best characteristic? Catalytic reaction under constant pressure needs pores structure with double pore sizes distributing: aperture of micropore is between λ and $\lambda/10$, aperture of macropore $\geq 10\lambda$. Here, λ is molecular mean free path,

$$\lambda = \frac{kT}{\sqrt{2}\pi\sigma^2 P} \tag{11}$$

T, temperature; k, Boltzmann constant ($1.3806 \times 10^{-23}\ J\ K^{-1}$); σ, effective diameter of molecule; and P, pressure.

In the reaction system of ethanol reforming: σCO_2 = 0.3941 nm, σCO = 0.3690 nm, σCH_4 = 0.3758 nm, σC_2H_5OH = 0.4530 nm, σH_2 = 0.2827 nm, σO_2 = 0.3467 nm, in which σCO_2 is the largest in products while σC_2H_5OH is largest in reactants. So, molecular CO_2 and C_2H_5OH could be only considered in ethanol reforming system to calculate the λ. The mean free path (λ) of molecular CO_2 and C_2H_5OH were calculated and shown in Table 4. The results showed that at 350 °C, the λ of ethanol is 93.2 nm, the λ of CO_2 is 123.0 nm, so catalysts' aperture size range of 12.3–93.2 nm were needed. T_2 sample with NiO grain size of 13.3 nm and Y_2O_3 of 76 nm was easy to form the pore at this range. And, at 350 °C, the WGS reaction can happen easily, so T_2 sample combined the WGS and reforming reaction very well, realizing no CO and high H_2 selectivity at last.

At 500 °C of reforming reaction, the λ of ethanol is115.6 nm, the λ of CO_2 is 152.7 nm, all of them are larger than at 350 °C, so the diffuse coefficient will turn large, the whole velocity of reaction

Table 1
Ethanol steam reforming products over sample T_2 at 350 °C for 79 h

T (h)	Selectivity (mol%)					Conversion (mol%)		Flow rate	
	H_2	CO	CH_4	CO_2	C_2	Ethanol	H_2O	Liquid income (ml min^{-1})	Gas outcome (ml S^{-1})
3	56.6		10.7	15.7	17.0				
4	58.6		12.8	19.1	9.5				
7.3	64.6		12.7	16.9	6.8				
8	64.5		12.6	16.4	6.5				0.04
14.3	50.3		7.0	10.8	31.8				0.09
15	68.7		12.1	20.2					
16	68.6		12.9	20.1				0.05	
20	68.7		12.9	21.1					0.05
22	66.2		12.6	21.2					
26	62.9		11.3	19.2	6.6				
38	66.8		10.0	16.1					0.06
41	65.2		12.3	22.5					0.04
50	65.0	0.5	12.3	22.2					0.04
60	60.1		10.8	17.2	11.8				0.06
65	61.1		12.5	24.3				0.2	0.23
70	62.3	0.4	12.1	22.8	2.8			0.3	0.38
75	64.0		12.8	23.4				0.4	0.42
79	64.9	0.4	12.7	22.0		98.6	87.9	0.5	0.38

Experimental conditions: mass of catalyst 4 g, H_2O/EtOH mol ratio R = 3:1, P = 1 atm.

Table 2
Ethanol steam reforming products over sample T_3 from 350 to 500 °C

Temperature (°C)	Time (h)	Selectivity (mol%)					Conversion (mol%)	Flow rate	
		H_2	CO	CH_4	CO_2	C_2	C_2H_5OH	Liquid income (ml min^{-1})	Gas outcome (ml S^{-1})
350	3	31.8	9.2	15.4	43.6				
	14	54.1	1.2	21.5	23.2			0.02	0.036
400	16	53.2	0.5	21.2	25.1		100		
	19	56.7		21.2	22.1				
450	23	45.5		27.3	27.2		100		
	28	47.1		25.6	27.3			0.05	0.056
	33	45.5		25.1	29.4				
	50	56.7		17.0	26.3			0.05	0.4
500	52	61.6		14.7	23.7		100		
	57	63.1		13.3	23.6			0.05	0.04

Experimental conditions: mass of catalyst 4 g, H_2O/EtOH mol ratio R = 3:1, P = 1 atm.

will be higher, the conversion of ethanol will be increased. However, when the heat-treated temperature is higher than 500 °C, the micropore of support will be sintered, only transition pore and macropore will be left, which leads to the decrease of catalyst selectivity.

From crystal grain sizes change, Tamman temperature of NiO is much lower than Y_2O_3, which claimed that during the reforming process Y_2O_3 was more stable than Ni(O). That was why the conversion of ethanol increased with the temperature, increasing obviously, but the selectivity of H_2 was not in high temperature steam reforming, which also proved that Ni(O) which favored for the break of bond C–C and C–H had been unstable at high temperature but Y_2O_3 which can promote O–H break were still stable.

3.3. Steady state reaction

Fig. 7 shows the effect of changing the flow rate on ethanol conversion over Ni/Y_2O_3 (a) and modified Ni/Y_2O_3 catalysts sample T_2

Table 3
Ethanol steam reforming products over sample T_5 from 350 to 500 °C

Temp (°C)	Time (h)	Selectivity (mol%)					Conversion (mol%)	Flow rate	
		H_2	CO	CH_4	CO_2	C_2	C_2H_5OH	Liquid income (ml min^{-1})	Gas outcome (ml S^{-1})
250	0.08	25.8	10.2	14.9	49.1			0.1	0.02
350	3.3	43.8	8.1	17.4	30.8			0.1	0.27
	6.3	50.7	9.8	21.1	18.4			0.1	0.21
400	8	56.8	6.3	19.7	17.2			0.1	0.42
	12	56.2	2.8	20.6	20.3			0.1	0.36
450	13.5	52.8	2.5	19.9	24.7		100	0.05	0.42
	15	51.9	2.0	20.5	25.6				
500	15.7	54.9	1.1	19.0	25.1		100	0.05	0.2
	20	55.0	0.6	17.S	26.6			0.05	0.03

Experimental conditions: mass of catalyst 4 g, H_2O/EtOH mol ratio R = 3:1, P = 1 atm.

Table 4
λ values of ethanol and CO_2 at different temperatures and relative catalyst aperture needed

Reaction temperature (°C)	Ethanol, λ (nm)	Micropore aperture (nm)	Macropore aperture (≥nm)	CO_2, λ (nm)	Micropore aperture (nm)	Macropore aperture (≥nm)
250	78.2	7.8–78.2	782	103.3	10.3–103.3	1033
350	93.2	9.3–93.2	932	123.0	12.3-123.0	1230
500	115.6	11.6–115.6	1156	152.7	15.3–152.7	1527
550	127.2	12.7–127.2	1272	168.0	16.8–168.0	1680
600	138.7	13.9–138.7	1387	183.2	18.3–183.2	1332
650	150.3	15.0–150.3	1503	198.5	19.9–198.5	1955
700	161.8	16.2–161.8	1618	213.8	21.4–213.8	2138
750	173.4	17.3–173.4	1734	229.1	22.9–229.1	2291
800	185.0	18.5–185.0	1850	244.3	24.4–244.3	2443

(b) in the absence of water vapor at 130 °C, as illustrated by the equation:

$$\ln\left(\frac{1}{1-x}\right) = k\frac{w}{F}, \tag{12}$$

where x is the degree of ethanol conversion (C_{EtOH}), w is the catalyst weight (150 mg), and F the flow rate (ml min^{-1}). For the catalysts a linear relationship can be observed between the degree of ethanol conversion and contact time, indicating a first-order reaction with respect to ethanol. The slope of each line denotes the rate constant k, which is found to be 2.95 (a), 4.27 (b) ml g^{-1} s^{-1} in the absence of water vapor, respectively. By the equation

$$\ln\frac{k_2}{k_1} = \frac{E_a}{R}\left(\frac{1}{T_1} - \frac{1}{T_2}\right), \tag{13}$$

where k is the rate constant (ml g^{-1} s^{-1}), R the gas constant (J K^{-1} mol^{-1}) and T the reaction temperature (K), the apparent activation energy of reaction E_a, can be computed, to be 7.04 kJ mol^{-1} (a) and 5.91 kJ mol^{-1} (b). This order is consistent with the order of constant k, which can also explain why sample T_2 had better activity in reforming reaction.

Thus, from the above results one can write the rate of reaction for ethanol over Ni/Y_2O_3 as

$$r = k[\text{ethanol}][H_2O]^n \tag{14}$$

where n needs to be determined. For all runs ethanol conversion was kept below 20% to assure operation in differential reactor conditions.

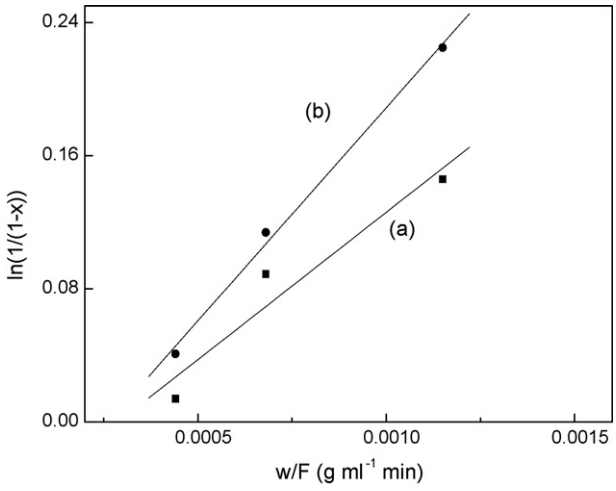

Fig. 7. Test of occurrence of first-order kinetics for ethanol reaction over Ni/Y_2O_3 (a), and modified Ni/Y_2O_3 sample T_2 (b) in gas concentrations: ethanol/N_2 (8.3%/91.7%). T = 130 °C, P = 1 atm.

3.4. TPD test

Fig. 8 presented t desorption profiles over T_2 sample Ni/Y_2O_3 catalyst, and showed the existence of three distinct temperature domains. Acetaldehyde (CH_3CHO, m/e = 29, 44, and 43) desorbed at three temperature domains of 120, 310, 650 °C with shoulder at 430 °C. Ethanol (C_2H_5OH, m/e = 31, 45, 29) desorbed in 120 °C, 650 °C. Methane (CH_4, m/e = 16, 15, 14) desorbed at 120, 320, 650 °C, carbon dioxide (CO_2, m/e = 44, 28) desorbed at same temperature domains with methane carbon monoxide (CO, m/e = 28, 14) desorbed at 120 and 650 °C. So, the initial mechanism of desorption of ethanol over modified catalyst Ni/Y_2O_3 could be ratiocinated and written as [6–8]:

$$CH_3CH_2OH \xrightarrow{-[H]} CH_3CH_2O_{(a)} \quad T_p = 120,\ 310,\ 650\,^\circ\text{C}$$

$$CH_3CH_2O \xrightarrow{-[H]} CH_3CHO_{(a)} \quad T_p = 120,\ 310, 650\,^\circ\text{C}$$

$$CH_3CHO_{(a)} \rightarrow CH_4 + CO_{(a)} \quad T_p = 120,\ 320, 650\,^\circ\text{C}$$

$$CO_{(a)} \xrightarrow{+[H_2O]} CO_2 + H_2 \quad T_p = 120,\ 320, 650\,^\circ\text{C}$$

The subscript (a) in the equation means active particles.

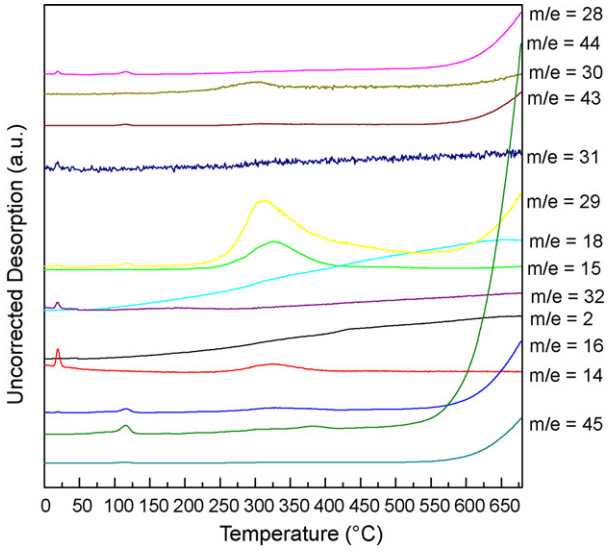

Fig. 8. Desorption products of ethanol over Ni/Y_2O_3 catalyst. Experimental conditions: mass of catalyst 100 mg, He as carrier gas flow rate 25 cm^3 min^{-1}, desorption temperature from 50 to 650 °C, vacuumize to 10^{-6} Torr.

4. Conclusions

Modification of heat treatment at 500 °C had a novel activation on catalyst Ni/Y_2O_3 to catalyze ethanol steam reforming with high H_2 yield 67.6% and no CO selectivity at 350 °C. Heat treatment had obvious effects on the grain size of active metal Ni(O) and aperture structure of catalyst Ni/Y_2O_3. The effects of sizes and aperture structure are important factors influencing the characteristics of catalysts. The low temperature (350 °C) activity, H_2 selectivity, CO elimination ability and stability of the catalysts followed the order: T_2 > unmodified Ni/Y_2O_3 > T_3 > T_5. The catalysts of Ni/Y_2O_3 are good choices to be used in ethanol steam reforming processors for fuel cell applications. These simple experiments also demonstrate that ethanol can be converted into H_2 simply and with high efficiency. Fast and efficient renewable fuel reforming is one of the critical steps in producing H_2 for fuel cells and the "hydrogen economy", and ethanol is now the most available and economical renewable fuel. This process just realizes the ideal of "Energy from nature, make the usage of energy more concordant with nature".

Acknowledgements

We acknowledge the financial support by NSFC Projects (No. 50606020) of China and ICD projects (Renewable energy No. 1).

References

[1] S. Freni, G. Maggio, S. Cavallaro, J. Power Sources 62 (1996) 67–73.
[2] G.A. Deluga, J.R. Salge, L.D. Schmidt, X.E. Verykios, Science 303 (2004) 993–997.
[3] H. Amandusson, L.G. Ekedahl, H. Dannetun, J. Catal. 195 (2000) 376–382.
[4] H. Amandusson, L.G. Ekedahl, H. Dannetun, Appl. Catal. A 217 (2001) 157–164.
[5] H. Amandusson, L.G. Ekedahl, H. Dannetun, J. Memb. Sci. 193 (2001) 35–47.
[6] A. Yee, S.J. Morrison, H. Idriss, J. Catal. 186 (1999) 279–295.
[7] A. Yee, S.J. Morrison, H. Idriss, Catal. Today 63 (2000) 327–335.
[8] A. Yee, S.J. Morrison, H. Idriss, J. Catal. 191 (2000) 30–45.
[9] F. Haga, T. Nakajima, K. Yamashita, S. Mishina, Nippon Kagaku Kaishi 1 (1997) 33–36.
[10] F. Haga, T. Nakajima, K. Yamashita, S. Mishina, Catal. Lett. 48 (1997) 223–227.
[11] F. Haga, T. Nakajima, K. Yamashita, S. Mishina, Nippon Kagaku Kaishi 11 (1997) 758–762.
[12] F. Haga, T. Nakajima, K. Yamashita, S. Mishina, Reaction Kinetics Catal. Lett. 63 (1998) 253–259.
[13] S. Freni, J. Power Sources 94 (2001) 14–19.
[14] S. Cavallaro, S. Freni, Int. J. Hydrogen Energy 21 (1996) 465–469.
[15] G. Maggio, S. Freni, S. Cavallaro, J. Power Sources 74 (1998) 17–23.
[16] S. Freni, S. Carvallaro, N. Mondello, L. Spadaro, F. Frusteri, Catal. Commun. 4 (2003) 259–268.
[17] F.J. Marino, E.G. Cerrella, S. Duhalde, Int. J. Hydrogen Energy 23 (1998) 1095–1101.
[18] F.J. Marino, M. Boveri, G. Baronetti, M. Laborde, Int. J. Hydrogen Energy 26 (2001) 665–668.
[19] A.N. Fatsikostas, D.I. Kondarides, X.E. Verykios, Chem. Commun. 9 (2001) 851–852.
[20] F. Auprêtre, C. Descorme, D. Duprez, Catal. Commun. 3 (2002) 263–267.
[21] J. Sun, X. Qiu, F. Wu, W. Zhu, J. Wang, Int. J. Hydrogen Energy 30 (2005) 437–445.
[22] J. Sun, X. Qiu, F. Wu, W. Zhu, W. Wang, S. Hao, Int. J. Hydrogen Energy 29 (2004) 1075–1081.
[23] A.N. Fatsikostas, X.E. Verykios, J. Catal. 225 (2004) 439–452.
[24] S.B. Wang, G.Q. Lu, Appl. Catal. 169 (1998) 271–280.
[25] E. Ruckenstein, Y.H. Hu, Appl. Catal. A 133 (1995) 149–161.
[26] J.B. Wang, Y.L. Tai, W.P. Dow, T.J. Huang, Appl. Catal. A 218 (2001) 69–79.
[27] Z.L. Zhang, X.E. Verykios, J. Chem. Soc. Chem. Commun. 1 (1995) 71–72.
[28] F. Auprêtre, C. Descorme, D. Duprez, Top. Catal. 30 (2004) 487–491.
[29] D. Duprez, Appl. Catal. 82 (1992) 111–157.
[30] J.R. Rostrup-Nielsen, J. Catal. 31 (1973) 173–179.
[31] D. Duprez, A. Miloudi, L. Tournayan, Appl. Catal. 14 (1985) 333–342.
[32] M.S. Batista, R.K.S. Santos, E.M. Assaf, J.M. Assaf, E.A. Ticianelli, J. Power Sources 124 (2003) 99–103.
[33] J. Rasko, A. Hancz, A. Erdohelyi, Appl. Catal. A 269 (2004) 13–25.
[34] J. Llorca, N. Homs, P. Ramirez de la Piscina, J. Catal. 227 (2004) 556–560.
[35] F. Frusteri, S. Freni, L. Spadaro, V. Chiodo, G. Bonura, S. Donato, S. Cavallaro, Catal. Commun. 5 (2004) 611–615.
[36] J. Barbier Jr., D. Duprez, Appl. Catal. B 3 (1993) 61–83.
[37] J. Barbier Jr., D. Duprez, Appl. Catal. B 4 (1994) 105–140.
[38] A.C.S.C. Teixeira, R. Giudici, Chem. Eng. Sci. 54 (1999) 3609–3618.
[39] C.L. Pieck, C.R. Vera, E.M. Peirotti, J.C. Yori, Appl. Catal. A 226 (2002) 281–291.
[40] J. Sehested, J. Catal. 217 (2003) 417–426.
[41] I. Aartun, T. Gjervan, H. Venvik, O. Görke, P. Pfeifer, M. Fathi, A. Holmen, K. Schubert, Chem. Eng. J. 101 (2004) 93–99.
[42] J. Sun, F. Wu, X. Qiu, F. Wang, S. Hao, Y. Liu, Chin. Catal. J. 25 (2004) 551–555.
[43] C. Sun, J. Sun, G. Xiao, H. Zhang, X. Qiu, H. Li, L. Chen, J. Phys. Chem. B 110 (2006) 13445–13452.